Neutral Sphingomyelinase 2

A Novel Target in Cigarette Smoke–Induced Apoptosis and Lung Injury

Simone Filosto[1], Sianna Castillo[1], Aaron Danielson[1], Lisa Franzi[1], Elaine Khan[1], Nick Kenyon[1], Jerold Last[1], Kent Pinkerton[2], Rubin Tuder[3], and Tzipora Goldkorn[1]

[1]Genome and Biomedical Sciences Facility (GBSF), Division of Pulmonary and Critical Care Medicine, University of California Davis, School of Medicine, Davis, California; [2]Department of Anatomy, Physiology and Cell Biology, School of Veterinary Medicine, University of California Davis, Davis, California; [3]Division of Pulmonary and Critical Care Medicine, University of Colorado Denver, School of Medicine, Denver, Colorado

Chronic obstructive pulmonary disease (COPD) is caused by exposure to cigarette smoke (CS). One mechanism of CS-induced lung injury is aberrant generation of ceramide, which leads to elevated apoptosis of epithelial and endothelial cells in the alveolar spaces. Recently, we discovered that CS-induced ceramide generation and apoptosis in pulmonary cells is governed by neutral sphingomyelinase (nSMase) 2. In the current experiments, we expanded our studies to investigate whether nSMase2 governs ceramide generation and apoptosis *in vivo* using rodent and human models of CS-induced lung injury. We found that exposure of mice or rats to CS leads to colocalizing elevations of ceramide levels and terminal deoxynucleotidyl transferase mediated X-dUTP nick end labeling–positive cells in lung tissues. These increases are nSMase2 dependent, and are abrogated by treatment with N-acetyl cysteine or anti-nSMase2 small interfering RNA (siRNA). We further showed that mice that are heterozygous for nSMase2 demonstrate significant decrease in ceramide generation after CS exposure, whereas acidic sphingomyelinase (aSMase) knockout mice maintain wild-type ceramide levels, confirming our previous findings (in human airway epithelial cells) that only nSMase2, and not aSMase, is activated by CS exposure. Lastly, we found that lung tissues from patients with emphysema (smokers) display significantly higher levels of nSMase2 expression compared with lung tissues from healthy control subjects. Taken together, these data establish the central *in vivo* role of nSMase2 in ceramide generation, aberrant apoptosis, and lung injury under CS exposure, underscoring its promise as a novel target for the prevention of CS-induced airspace destruction.

Keywords: neutral sphingomyelinase2; ceramide; apoptosis; chronic obstructive pulmonary disease; mouse model

Cigarette smoking is associated with 80–90% of the chronic obstructive pulmonary disease (COPD) cases in the United States (1). Active exposure to cigarette smoke (CS) also contributes to the increased incidence of related pulmonary diseases such as asthma, bronchitis and pulmonary fibrosis. However, COPD is considered to be the prototypical CS-related disorder, and is characterized by chronic inflammation of the airways and severe damage to the lung parenchyma, leading to pulmonary emphysema.

Several mechanisms have been proposed to be involved in the pathogenesis of pulmonary emphysema, including an imbalance of proteases and antiproteases, and oxidative stress (2). Recent studies suggest another mechanism involved in the development of pulmonary emphysema: apoptosis of alveolar wall cells (3). An increase in apoptotic alveolar epithelial and endothelial cells in the lungs of patients with COPD was detected, thus leading to the net outcome of loss of alveolar units leading to emphysema.

Recent studies in a novel mouse model of targeted endothelial cell apoptosis have demonstrated emphysematous-like changes associated with up-regulation of ceramide consistent with the observations in patients with COPD (4, 5). These authors used the model of vascular endothelial growth factor receptor blockade and reported increased ceramide in lung endothelial cells, which was critical in activating cell death, oxidative stress, and emphysema (5). These results were prevented by fumonisin B1 (inhibitor of the *de novo* ceramide synthesis pathway, suggesting that ceramide synthase could be involved in the modulation of ceramide levels in that model. Another report demonstrated that superoxide dismutase protected against apoptosis and alveolar enlargement induced by ceramide (6).

Ceramide was also suggested to injure pulmonary endothelial and hepatic cells during sepsis (7). Another study, based again on the protective effects of fumonisin B1 in a guinea pig asthma model, also proposed a role for increased ceramide-mediated oxidative stress in the pathogenesis of asthma (8). Teichgraber and colleagues (9) and Hamai and colleagues (10) have recently reported that ceramide accumulation mediates inflammation, cell death, and infection susceptibility in cystic fibrosis.

If, indeed, ceramide is a critical pathogenic element in lung injury processes, such as emphysema, then it is important to elucidate the exact cellular mechanism that leads to excess generation of ceramide under CS exposure. Ceramide levels are elevated in situations associated with cellular stress, such as ischemia, radiation, and exposures to chemotherapeutic agents or oxidative stress (11), and ceramide increase has previously been shown to be crucial in the induction of programmed cell death (apoptosis) (12). Because ceramide is a second messenger molecule that modulates cell apoptosis (13–18) and oxidative stress (16), others and we have proposed that ceramide up-regulation may induce lung epithelial destruction, as presented in the pathogenesis of several lung injury diseases (3, 16, 19). Recent reports provide a very strong case for cell death (apoptosis) having a major role in lung injury in several pulmonary diseases, such as asthma, bronchitis, and COPD (1, 3, 5, 20–22). In simple terms, loss of cells by augmented apoptosis would be expected to be involved, or perhaps initiate, the overall tissue destruction responsible for lung injury (21, 22).

Ceramide can be generated *de novo* by acylation of sphingosine or in the reverse pathway of sphingomyelin hydrolysis by sphingomyelinase (SMase) isoenzymes. According to current models, sphingomyelin may be constitutively metabolized to ceramide by several SMases, but some SMases may have special pathophysiological significance (23). Others and we have reported that the major SMase isoenzyme that becomes activated

(*Received in original form November 10, 2009 and in final form March 23, 2010*)

This work was supported by National Institutes of Health (NIH) grants HL-71871 and HL-66189 (T.G.) and Tobacco-Related Disease Research Program (TRDRP) grant 17RT-0131 (T.G.), and, in part, by NIH grants NHLBI K08 HL-076415, and NCRR UL1RR024146, a component of the National Institutes of Health Roadmap for Medical Research.

Correspondence and requests for reprints should be addressed to Tzipora Goldkorn, Ph.D., Signal Transduction, UC Davis, School of Medicine, Genome and Biomedical Sciences Facility, Room 6321, 451 Health Sciences Drive, Davis, California, 95616. E-mail: ttgoldkorn@ucdavis.edu

Am J Respir Cell Mol Biol Vol 44. pp 350–360, 2011
Originally Published in Press as DOI: 10.1165/rcmb.2009-0422OC on May 6, 2010
Internet address: www.atsjournals.org

by oxidative stress appears to be neutral SMase (nSMase) 2 (or sphingomyelin phosphodiesterase 3 [SMPD3 gene]), which is expressed in the Golgi, but probably also in the plasma membrane. Our studies in human airway epithelial (HAE) cells (human bronchial epithelial 1 [HBE1] papilloma virus–immortalized cells) demonstrated that CS stimulates ceramide generation, which leads to elevation of apoptotic events via the specific activation of nSMase2 (19). We therefore attempted to determine *in vivo* the specific component in the ceramide-generating machinery that is activated by CS exposure, which could present an important novel target for pharmacologic intervention in lung injury diseases. Thus, we designed studies to investigate whether CS can affect ceramide levels and apoptosis in the lungs of mice and rats, and what role is played by nSMase2 in CS-induced lung injury and apoptosis in these animal models.

MATERIALS AND METHODS

Animal Studies

All procedures were performed in accordance with an institutional animal care and use committee–approved protocol. All animals were maintained in a high efficiency particulate air (HEPA)-filtered laminar flow cage rack with a 12-hour light/dark cycle and allowed free access to food (Purina Rodent Chow; Ralston-Purina. Canada, Woodbridge, Ontario) and water before experiments. Animals were housed and cared for by the veterinary staff of Animal Resource Services at University of Colorado Davis in Association for Assessment and Accreditation of Laboratory Animal Care (AAALAC)-accredited facilities, and were routinely screened for health status by serology and histology by the veterinary animal resources facility. In a series of experiments, 10- to 20-week-old 129/Sv and C57BL/6 mice, and then spontaneously hypertensive rat (SHR)/NCrIBR (strain code from Charles River Laboratory, Inbred; Wilmington, MA), were used in this research. To investigate the role of oxidative stress–mediated lung injury, mice were exposed (or not) to 60 mg/m^3 CS of TSP, for 6 h/d, 5 d/wk, and fed either a chow diet or a diet supplemented with N-acetyl cysteine (NAC) (0.4%). Mice exposed to either filtered air or CS (research cigarettes) were killed within 6 weeks after the exposures started. Rats were CS exposed (same conditions as mice) until 14 weeks in Dr. Pinkerton's laboratory. Intratracheal instillation of lipid analogs (C6-ceramide and -dihydroceramide: 1 mg/kg) was done by solubilization in ethanol, followed by delivery at the base of the protruded tongue in 80–100 μl of perflourocarbon (1:5, vol/vol). Control mice were instilled with perflourocarbon-1% ethanol, and 1% BSA. Local RNA interference with nSMase2 siRNA or scrambled iRNA was performed, as reported by Zhang and colleagues. (24), by intranasal installation of biotin-labeled nSMase2 siRNA, which had been specially synthesized for our laboratory (by Dharmacon, Lafayette, CO). Acidic SMase (aSMase) knockout (KO) mice (C57BL/6 background) came from E. H. Schuchman, Mount Sinai Medical Center (New York, NY). Heterozygous nSMase2 (nSMase2$^{-/+}$) mice (129/Sv background) came from Dr. Jean Jaubert, Pasteur Institute (Paris, France).

In this study, a total of 90 129/Sv mice and 156 C57BL/6 mice were used. Six 129/Sv mice for each time/treatment point were exposed, or not, to CS for 1 day, 3 days, 1 week (5 d of exposure), or 3 weeks; six C57BL/6 mice for each time/treatment point were exposed, or not, to CS and fed, or not, with 0.4% NAC, and killed after 1–6 weeks. Two 129/Sv mice for each time/treatment point were instilled, or not, with C6-ceramide or C6-dihydroceramide; 16 129/Sv mice (2 for each time/treatment point) were used for the nSMase2 siRNA experiments; 4 aSMase KO (aSMase$^{-/-}$) mice and 4 nSMase2$^{-/+}$ mice for each time/treatment point were exposed, or not, to CS for 1 or 3 weeks. Six rats for each time/treatment point were exposed, or not, to CS, and killed weekly for up to 14 weeks.

Human Lung Samples

Human lung sections were provided by Dr. Rubin Tuder, University of Colorado (Denver, CO). Lung slides from six different control lungs were compared with lung slides of six different patients with emphysema (smokers). The emphysema lung sections came from 49- to 54-year-old male and female patients, all diagnosed with severe centrilobular emphysema, except for one diagnosed with mild emphysema. The control lung sections came from 28- to 75-year-old male and female patients with no diagnosed lung pathologies or with non–emphysematous-like diagnosed diseases, such as bronchoalveolar carcinoma–mucinous type, neuroendocrine tumor (carcinoid tumor), or invasive moderated differentiated adenocarcinoma.

Determination of Cellular Ceramide Levels by Diacylglycerol Kinase Assay

Ceramide was quantified by the diacylglycerol kinase assay, as previously described (14, 15). Briefly, frozen lung fragments were thawed and weighed. After destruction of the tissue in ice-cold PBS solution with an electric homogenizer, lipids were extracted with methanol:chloroform:1 N HCl (100:100:1, vol/vol/vol). The lipids in the organic phase were dried under reduced pressure, and were resuspended in 100 μl of the reaction mixture, containing [γ-P^{32}] ATP, and incubated at room temperature (RT) for 1 hour. The reactions were terminated by extraction of lipids with 1 ml of methanol:chloroform:1 N HCl, 170 μl of PBS, and 30 μl of 0.1 M EDTA. The lower organic phase was dried under reduced pressure, and the lipids were resolved by thin-layer chromatography on silica gel 60 plates (Whatman, Piscataway, NJ) using a solvent of chloroform: methanol:acetic acid (65:15:5, vol/vol/vol). Ceramide 1–phosphate was detected by autoradiography, and incorporated ^{32}P was quantified by densitometry scanning using a Molecular Dynamics scanner (GE Healthcare, Piscataway, NJ). The amount of ceramide was normalized per protein unit of the tissue.

Immunohistochemistry

Paraffin-embedded tissue sections were deparaffinized with xylene washes and rehydrated with several washes in ethanol/water solutions. Antigen retrieval was facilitated by incubation of sections for 10 minutes at 95°C in a 100-mM citrate buffer solution (pH 6). Tissue was blocked in 10% goat serum, 1% BSA in PBS. Primary antibodies (or preimmune rabbit sera) were incubated at RT for 2 hours in the blocking solution. These antibodies included: anti-nSMase2 rabbit (1:50), generated against a partially purified nSMase2; anti-ceramide (1:20), from Alexis Biochem (Enzo Life Sciences, Plymouth Meeting, PA); and anti-ceramide, rabbit IgG (1:50), kindly provided by Dr. Erhard Bieberich (25), Medical College of Georgia (Augusta, GA). In negative control, the primary antibody incubation was omitted. After three washes in PBS, secondary antibodies were incubated for 1 hour at RT (anti-rabbit or mouse IgG [1:200 diluition], Alexa Fluor 488 or 555 dyes). Nuclei were stained by incubating tissue with 4′,6-diamidino-2-phenylindole (100 ng/ml in PBS) for 5 minutes at RT. Sections were mounted with fluoromount-G (Southern-Biotech, Birmingham, AL) and images were taken at 200× or 400× magnification (20× air or 40× oil objectives) with an LSM 5 Pascal Zeiss laser scanning confocal microscope (Standort Göttingen, Vertrieb - Germany or an Olympus FluoView FV1000 confocal microscope (Center Valley, PA. The laser excitation and the camera sensitivity were regulated according to the stain of the negative control (i.e., mean intensity of the fluorochromes was detected as null in the negative control). Staining levels from randomly acquired images were scored by four people independently and/or quantified by software analysis.

Evaluation of Fragmented DNA by Terminal Deoxynucleotidyl Transferase–Mediated X-dUTP Nick End Labeling Assay

Paraffin-embedded tissue sections were deparaffinized and rehydrated as described for immunohistochemistry (IHC). Fragmented/apoptotic nuclei were stained by terminal deoxynucleotidyl transferase–mediated X-dUTP nick end labeling (TUNEL) assay following the protocol described in the manufacturer's instruction (Roche, Tucson, AZ) with an enzymatic reaction of 45 minutes at 37°C. A 5-minute incubation at RT with 4′,6-diamidino-2-phenylindole in PBS (100 ng/ml) was used to stain all of the nuclei. Colocalization with nSMase2 antibody was performed by combining the protocol of the TUNEL assay (done first) with the IHC protocol. Sections were mounted with fluoromount-G, and images were taken at 200× or 400× magnification with an LSM 5 Pascal Zeiss laser scanning or an Olympus FluoView FV1000 confocal microscope.

Quantitative Real-Time Reverse Transcriptase PCR (qRT-PCR)

RNA was isolated using Trizol reagent (Invitrogen, Carlsbad, CA), according to the standardized extraction protocol supplied by the

manufacturer. Total RNA was converted to cDNA using oligo-dT primers and MuMLV-reverse transcriptase (Promega, Madison, WI), following the instruction of the manufacturer. Quantitative PCR was performed on an ABI PRISM 7900HT Sequence Detection System (Applied Biosystem, Carlsbad, CA) using Syber green qPCR Supermix (Invitrogen) and specific primers for murine nSMase2 (TGAAAGAG CAGCTACACGGCTA; GAGACCGCTGTTGAGACATTTG) and glyceraldehyde 3-phosphate dehydrogenase (CTGCACCACCAACT GCTTAG; GATGGCATGGACTGTGGTC). Reactions were performed in triplicate for each sample. The cycle times for nSMase2 were normalized to that for glyceraldehyde 3-phosphate dehydrogenase.

Immunoblotting

Protein samples were separated on 10% or 15% acrylamide SDS-page or 5–15% gradient gel (BioRad) at 80–100V before transfer to nitrocellulose membrane (20-μM pore; Bio-Rad) in Tris/glycine buffer at 100 V for 60 minutes at 4°C. Membranes were blocked in 5% milk in 0.1% Tris-buffered saline/Tween 20 (TBST) and probed with primary antibody for 2–4 hours at RT (anti-nSMase2, 1:1,000, generated in rabbit against a partially purified nSMase2; anti–caspase-3, 1:1,000 from Cell Signaling [Danvers, MA]; anti–β-actin 1:5,000 from Sigma [St. Louis, MO]). Membranes were washed (three times with TBST), probed with horseradish peroxidase (HRP)–conjugated secondary antibody (1:7,500 mouse or rabbit in 5% nonfat dry milk) for 90 minutes at RT, and washed (three times with TBST). Proteins were visualized by enhanced chemiluminescence (Pierce, Rockford, IL). Data analysis and quantification were done using ImageJ 1.41 software (National Institutes of Health, Bethesda, MD).

Hematoxylin and Eosin Stain

Staining was performed by standard procedures on lung sections after sample fixation, dehydration, and embedding in paraffin. Images were acquired by optical microscopy at 200× magnification.

RESULTS

CS Induces Accumulation of Ceramide in Lungs of 129/Sv or C57BL/6 Mice

Consistent with our previous observations in HAE cells exposed to oxidative stress via CS treatment (16, 19), we found that ceramide is accumulated in the lungs of mice during exposure to CS (Figure 1). Figure 1 demonstrates a twofold increase of ceramide levels in the lungs of 129/Sv mice exposed to CS for 1 week as compared with control mice exposed to fresh air. The quantization of ceramide levels was performed by lipid extraction from the respective lung tissues, followed by the assessment of ceramide using the diacylglycerol kinase assay, which was normalized per protein unit of the tissue (Figure 1A). In addition, as shown in Figure 1B, IHC of lung tissues from the same groups of mice demonstrated ceramide accumulation (stained with an anti-ceramide antibody) in the CS-exposed group of mice in comparison to the controls (air exposed). Although 129/Sv mice responded to CS with significantly increased ceramide generation after 1 week of exposure, the C57BL/6 strain demonstrated a slower response, and showed a measurable increase in ceramide levels starting only from the third week of CS exposure. Figure 1C shows overall lung histology of 129/Sv mice exposed (or not) to CS for 1 week.

C6-Ceramide, but Not C6-Dihydroceramide, Increases Ceramide in Lungs of 129/Sv Mice

It is well known that synthetic membrane-permeant ceramide analogs, such as C6-ceramide, can mimic the effects of endogenous ceramide via a positive stimulation of the ceramide-generating machinery (14, 15, 26). The functional effects of exogenously administrated short-chain ceramides were explained by their stimulation of endogenous ceramide production (16, 17). At the same time, the dihydro forms of the analogs, like C6-dihydroceramide, are inactive. They are not able to induce an increase in endogenous ceramide levels, and, therefore, cannot mimic stress responses (27). Indeed, we demonstrated in our previous studies, in HAE cells, that treatment with the C6-ceramide analog, but not with the C6-dihydro derivative increased the cellular levels of ceramide and apoptosis (16, 17). The importance of this stimulus is in starting a positive feedback loop of ceramide production, allowing for augmentation of ceramide generation and lung injury.

Thus, we tested whether direct intratracheal instillation of ceramide analogs can recapitulate the phenotype of the CS exposure, namely, elevation of endogenous ceramide levels. 129/Sv mice were instilled with either C6-ceramide or C6-dihydroceramide, then killed 24 hours later, and assayed by IHC for the amount of ceramide in the respective lungs. As shown in Figure 1D, the instillation of C6-ceramide analog indeed caused ceramide accumulation in the lung, whereas the administration of C6-dihydroceramide did not elicit ceramide increase, indicating that the ceramide machinery *in vivo* has similar responses to those observed earlier in cells, *in vitro*. Furthermore, C6 ceramide analog enhanced endogenous ceramide generation (Figure 1D) at comparable levels to those induced by CS exposure (Figure 1B), whereas dihydroceramide did not augment ceramide levels. Increased endogenous ceramide levels were reported previously by Petrache and colleagues (5), who instilled the C12-ceramide analog intratracheally into rats. In this study, most of the increase in the endogenous ceramide was observed in the endothelial cell population.

Ceramide Generation and DNA Fragmentation in the Lungs of Mice Exposed to CS

Ceramide accumulation may play a crucial role in the induction of stress-stimulated apoptosis in the lung (5, 19, 28, 29). We reported previously that ceramide production is responsible for apoptosis induction in HBE1 and A549 adenocarcinoma cells exposed to H_2O_2 or to CS, and that ceramide generation in these cells is upstream of caspase cascades (16, 17, 19). Here, we attempted to verify whether any correlation between ceramide generation and apoptosis induction exists also in the lungs of mice exposed to CS.

To detect fragmentation of DNA, TUNEL assays were performed on lung sections from 129/Sv or C57BL/6 mice exposed for several weeks to CS. Figure 2A demonstrates an increase in TUNEL-positive cells in lung sections of C57BL/6 mice exposed to CS for 4 weeks. Mice that were exposed to filtered air or those exposed to CS presented major differences in TUNEL staining, and the observed fragmentation of DNA colocalized with ceramide accumulation.

nSMase2 Expression Colocalizes with TUNEL-Positive Cells Both in the Bronchial Epithelium and Alveolar Septal Cells in Lungs of Mice Exposed to CS

We have previously shown in HAE cells that nSMase2 is the sole target that is activated by CS exposure in the ceramide-generating machinery (19). Here, we show, for the first time, that nSMase2 is also being overexpressed in the lungs of mice exposed to CS. C57BL/6 mice presented a significant increase in nSMase2 protein expression after 3–4 weeks of exposure to CS, whereas 129/Sv mice displayed augmented expression of nSMase2 as early as only 1 week after CS exposure.

As shown in Figure 2B, lung sections from CS-treated mice presented augmented nSMase2 expression, and nSMase2 appeared to be overexpressed in both bronchial epithelium and alveolar septal cells. Importantly, at the same respective times of CS exposures, increases in TUNEL-positive cells were also observed, suggesting that nSMase2 overexpression, ceramide

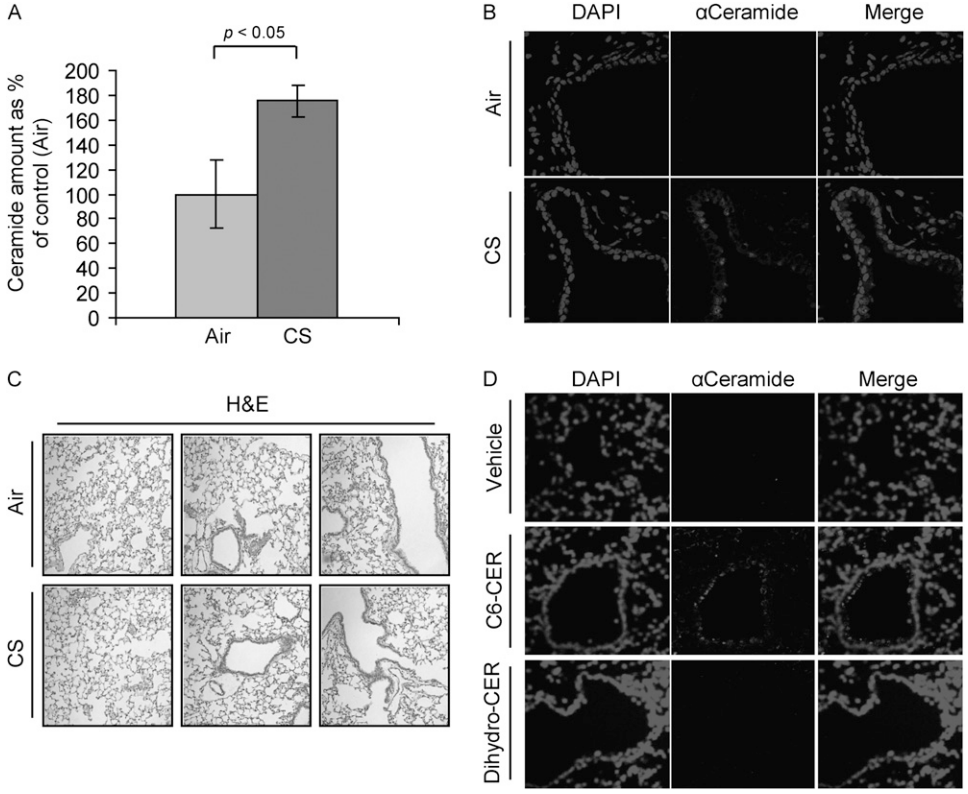

Figure 1. Cigarette smoke (CS) induces ceramide generation in the lung. Three 129/Sv mice for each time/treatment point were exposed, or not, to CS for 1 week (*A* and *B*), whereas two 129/Sv mice for each treatment/point were intratracheally instilled with ceramide analogs or BSA (vehicle) (*D*). The mice were killed and assayed for ceramide levels in the lung by diacylglycerol kinase assay (*A*) and immunohistochemistry (IHC) (*B* and *D*). (*A*) The amount of ceramide in the graphic represents the average of three independent experiments (three mice per treatment), and is reported as percentage of the untreated mice (filtered air) after normalization per protein unit of the tissue; the *P* value in (*A*) was obtained by Student's *t* test per number of mice. (*B*) Total nuclei (*left panels*) were stained by 4′,6-diamidino-2-phenylindole (DAPI ceramide (*central panels*) was localized by incubating lung slides with a specific anti- (α) ceramide antibody (Ab) and stained by Alexa Fluor 555 dye–conjugated Ab; the *panels on the right* show the merges of total nuclei and ceramide staining. (*C*) Hematoxylin and eosin (H&E) stain of the 129/Sv mice exposed, or not, to CS for 1 week. (*D*) mice were instilled with synthetic lipids, either C6-ceramide (C6-CER) or dihydro-C6-ceramide (Dihydro-CER), killed 24 hours after instillation, and assayed for ceramide levels in the lung by IHC: ceramide (*central panels*) was localized as in (*A*) and stained by Alexa Fluor 555 dye; total nuclei were stained by DAPI (*left panels*); merge images of ceramide and nuclei staining are shown (*right panels*). Images were acquired with an LSM 5 Pascal Zeiss laser scanning or an Olympus FluoView FV1000 confocal microscope.

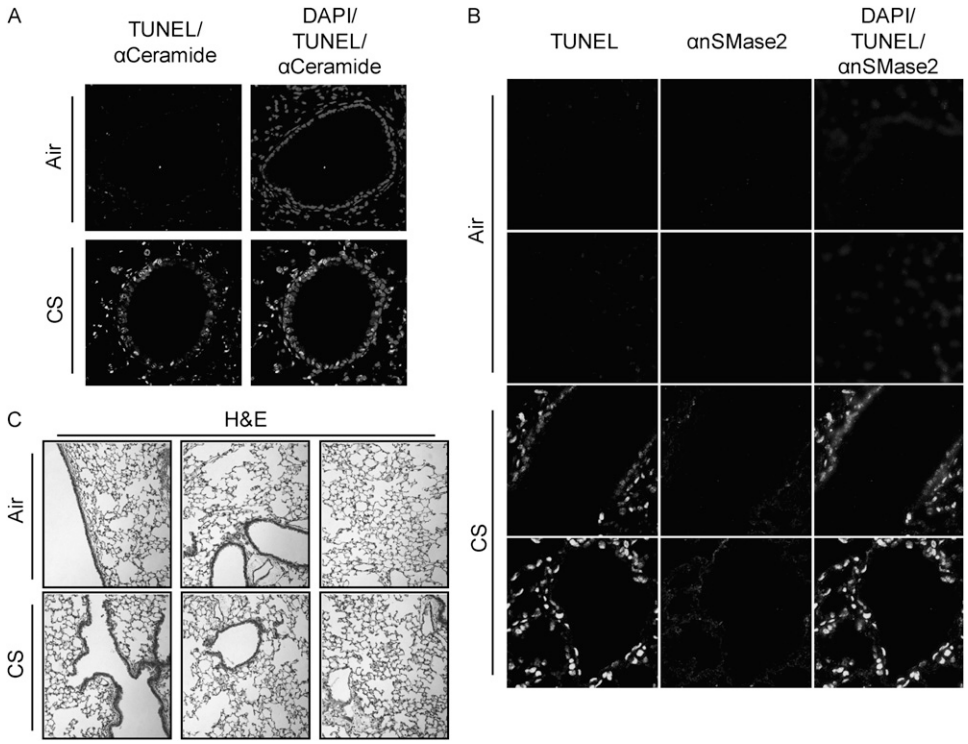

Figure 2. Ceramide generation, neutral sphingomyelinase (nSMase) 2 overexpression, and DNA fragmentation are strictly related in lungs of CS-exposed mice. (*A*) C57BL/6 mice were exposed, or not, to CS for 4 weeks, then killed and assayed for ceramide levels by IHC, as in Figure 1 and fragmented DNA by terminal deoxynucleotidyl transferase–mediated X-dUTP nick end labeling (TUNEL) assay (*brighter stain*); total nuclei were also stained by DAPI, as in Figure 1. The *left panel* shows the merge between fragmented DNA and ceramide staining, whereas the *right panel* presents the merge of total nuclei, fragmented DNA (*brighter stain*), and ceramide localization. (*B*) Mice were exposed, or not, to CS for 5 weeks, killed, and tested for fragmented DNA as in (*A*) (*stain* in *left panels*) and nSMase2 expression (*stain* in *second panels from the left*) by incubating lung slides with a specific anti- (α) nSMase2 Ab, and staining it by Alexa Fluor 555 dye. Total nuclei were stained by DAPI (not shown alone); *right panels* show the merge of TUNEL (*brighter stain*), αnSMase2, and DAPI. (*C*) H&E stain (overall lung histology) of the C57BL/6 mice exposed, or not, to CS for 5 weeks.

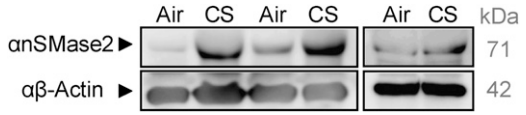

Figure 3. nSMase2 is overexpressed in 129/Sv mice after 1 week of exposure to CS. Three 129/Sv mice were exposed, or not, to CS for 1 week, then killed, and assayed by immunoblotting (IB) for the levels of nSMase2 expression in the whole-lung lysates (lung tissues homogenized in the presence of 0.4% Triton-X 100). Total protein (200 μg) from each lung was separated on SDS-PAGE and immunoblotted using specific αnSMase2 and αβ-actin antibodies. Each sample in the figure represents a different mouse. Separate *panels* represent two different Western blot analyses.

generation, and DNA fragmentation are all synchronized and colocalized. Figure 2C shows just the overall lung histology of C57BL/6 mice exposed, or not, to CS for 5 weeks.

Furthermore, Figure 3 shows by immunoblotting that nSMase2 is overexpressed in the whole lung lysate of three different 129/Sv mice after 1 week of exposure to CS.

NAC Counteracts nSMase2 Overexpression and Apoptosis Induced by CS in Mice

NAC is a well characterized antioxidant that is able to neutralize the effects of oxidative stress, both in cell lines and in rats and mice (30, 31). NAC is rapidly metabolized to intracellular glutathione (GSH), which is the main antioxidant produced by the cells. We have shown previously in HAE cells that CS produces reactive oxygen species (ROS), such as H_2O_2, which induce ceramide generation and apoptosis. Furthermore, others and we have shown that both GSH and NAC can quench ceramide production and apoptosis induction in these cultured cells (16, 32).

As shown in Figure 4A, 4 weeks of CS exposure increased the expression of nSMase2 in C57BL/6 mice, and also elevated the number of TUNEL-positive cells (Figure 4B). However, control mice exposed to filtered air, or mice exposed to CS for the same time period but supplemented with 0.4% NAC in their diet, showed a significant reduction in nSMase2 staining and TUNEL-positive cells. nSMase2 expression and TUNEL-positive cells were quantified by densitometric software analysis of randomly acquired images from lung slides of three different mice: the quantifications are reported as histograms in Figures 4C and 4D.

Considering that the TUNEL staining may not accurately represents apoptosis (33), we estimated the level of cleavage/activation of caspase-3 in the whole-lung homogenates of the mice. This cleavage is a specific marker for the execution phase of apoptosis. As shown in Figure 5, CS exposure increased the cleaved caspase-3 levels in comparison to control (air-exposed mice), and the NAC diet could reduce such increase. These data indicate that NAC diet may exert antiapoptotic effects in the

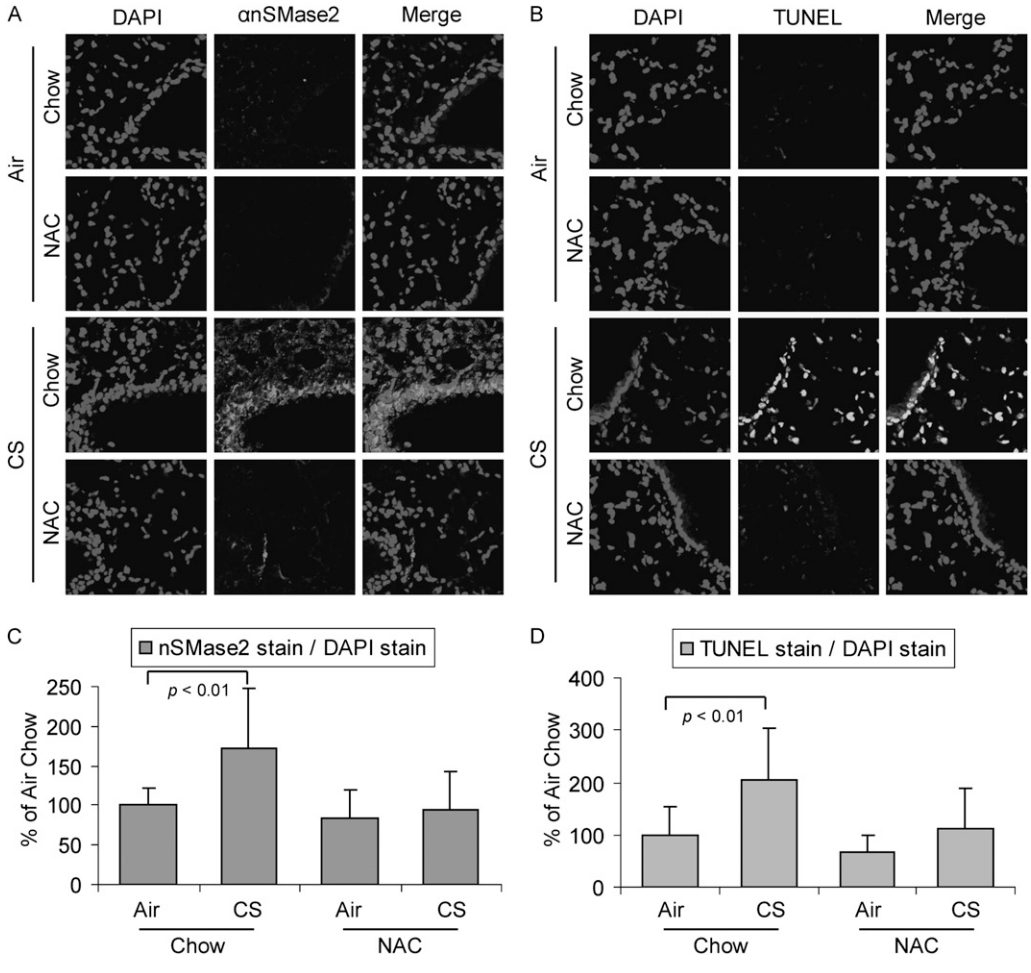

Figure 4. N-acetyl cysteine (NAC) counteracts nSMase2 overexpression and DNA fragmentation induced by CS. Three C57BL/6 mice were exposed, or not, to CS for 4 weeks, and fed, or not, with a 0.4% NAC–enriched diet, then killed, and assayed by IHC for nSMase2 expression (*A*) or by TUNEL staining for detection of fragmented DNA (*B*). Total nuclei were stained by DAPI (*left panels*); nSMase2 was stained by Alexa Fluor 555 dye (*central panels* in [*A*]); TUNEL-positive cells are in *central panels* in [*B*]; respective merge images are shown in the *right panels*. (*C*) A total of 12 random images were acquired at 200× magnification from lung sections of three different mice per each treatment (four images per each mouse) and the mean intensity of nSMase2 stain (analyzed by LSM 5 Pascal 4.2 software) was normalized to the mean intensity of DAPI stain (proportional to cell nuclei/number) in each image; then, the average value of nSMase2 stain from the air/chow–treated mice was arbitrarily set as 100% value, and all other values (means and SD) have been adjusted accordingly. (*D*) TUNEL stain in the lung sections was quantified as described above in (*C*) and reported as means (±SDs). The *P* values in (*C*) and (*D*) were obtained by Student's *t* test per number of images.

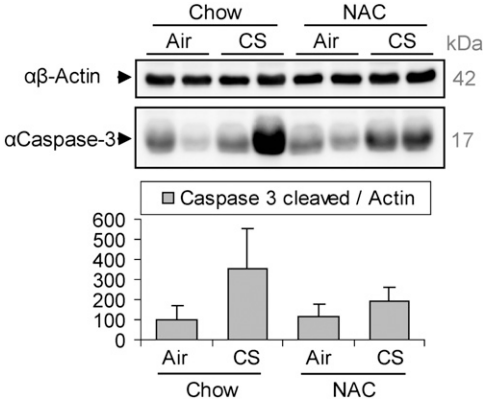

Figure 5. CS induces caspase-3 activation, which is reduced by NAC. Three C57BL/6 mice were exposed, or not, to CS for 5 weeks, and fed, or not, with a 0.4% NAC enriched diet, then killed, and assayed by IB for the activation of caspase-3 (presence of cleaved caspase-3) in the whole-lung homogenates. The image shows samples of 200 μg total proteins from lungs of two different mice per treatment. The samples were separated on SDS-PAGE and immunoblotted using specific αβ-actin and αcaspase-3 antibodies. The histogram below shows the quantification (by densitometry) of the levels of caspase-3 cleaved normalized to the respective levels of β-actin in the lungs of three different mice.

lung, probably counteracting the oxidative stress induced by CS, thereby reducing the expression of nSMase2 and ceramide generation followed by apoptosis inhibition.

In Vivo siRNA Silencing of nSMase2 in 129/Sv Mice

We compared our findings of silencing nSMase2 in cell culture (19, 29) with *in vivo* silencing studies, as described by Zhang and colleagues (24), by administrating biotin-labeled nSMase2 siRNA, which had been specially synthesized for our laboratory. As shown in Figure 6A, 129/Sv mice were administered intranasal murine nSMase2 siRNA (2 mg/kg of body weight) for the indicated time points. nSMase2 message levels were determined. We found that nSMase2 siRNA inhibited nSMase2 message in a time-dependent manner (RT-PCR) in the mouse lung. Then, as shown in Figure 6B, lung sections were incubated with peroxidase-labeled streptavidin and 3,3′-diaminobenzidine substrate to assess the presence of biotin (brown staining), which indicates the presence of nSMase2 siRNA (found both the in airway and in alveoli). Finally, as shown in Figure 6C, lung sections were processed for ceramide staining (arrows indicate representative ceramide-positive cells) after instillation of the murine nSMase2 siRNA. As shown, treatment with nSMase2 siRNA significantly reduced the number of ceramide-positive cells (Figure 6C, lower panels) compared with mice subjected to CS alone, and as compared with mice administered nonspecific siRNA and also subjected to CS (Figure 6C, upper panels). This is a very important finding, because mice instilled with a scrambled vector still showed significant positive staining, both for ceramide and nSMase2, in lung sections after CS exposure.

CS Exposures of nSMase2$^{-/+}$ and aSMase$^{-/-}$ Mice

129/Sv wild-type (WT) and C57BL/6 WT mice were exposed to filtered air or to CS for 3 weeks. In parallel, aSMase$^{-/-}$ mice (C57BL/6 background) and the nSMase2$^{-/+}$ mice (129/Sv background) were also exposed to these treatments for the same duration. Figure 7 shows that the mice with the aSMase gene knocked out (Figure 7A, lower panels) generated the same levels of ceramide in response to CS as the respective WT mice (Figure 7A, upper panels), as also reflected by the quantitative analysis in

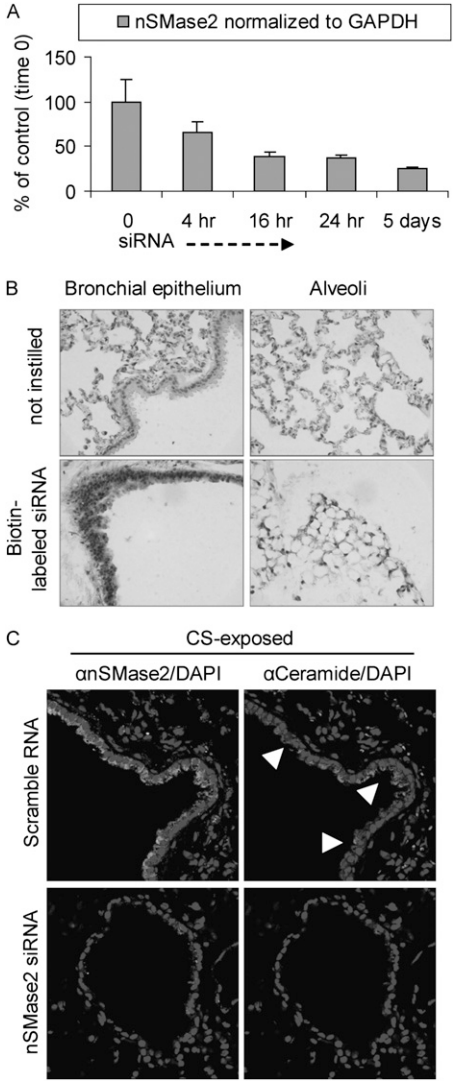

Figure 6. Small interfering RNA (siRNA) of nSMase2 in the lung prevents ceramide accumulation during CS exposure. Two 129/Sv mice for each time/treatment point were instilled for up to 5 days with biotin-labeled nSMase2 siRNA or scrambled RNA, while exposed in parallel to CS. (*A*) nSMase2 expression in siRNA-silenced lungs was evaluated by RT-PCR in triplicate samples and normalized to the level of glyceraldehyde 3-phosphate dehydrogenase (GAPDH). (*B*) Lung sections from 5-day-instilled mice were incubated with peroxidase-labeled streptavidin and 3,3′-diaminobenzidine (DAB) substrate to assess the presence of biotin (*darker staining*), which indicates the presence of siRNA both in airway and in alveoli (*left* and *right panels*, respectively); images were acquired by optical microscopy. (*C*) Lung sections from mice instilled with nSMase2 siRNA for 5 days, or instilled with scrambled RNA, were subjected to IHC using specific αnSMase2 (*brighter stain* in *left panels*) and αceramide (*brighter stain* in *right panels*) antibodies; total nuclei were stained by DAPI; *arrowheads* indicate examples of ceramide accumulation–positive cells. Fluorescent images were acquired with an Olympus FluoView FV1000 laser scanning confocal microscope and show the respective merges of nSMase2/nuclei and ceramide/nuclei stains in mice instilled with either scrambled siRNA (*upper panels*) or nSMase2 siRNA (*lower panels*).

Figure 7C. In contrast, the nSMase2$^{-/+}$ mice displayed a much lower ceramide level (Figure 7B, lower panels) compared with the respective WT mice upon CS exposure (Figure 7B, upper panels), as also demonstrated by the statistical analysis in Figure 7D. These

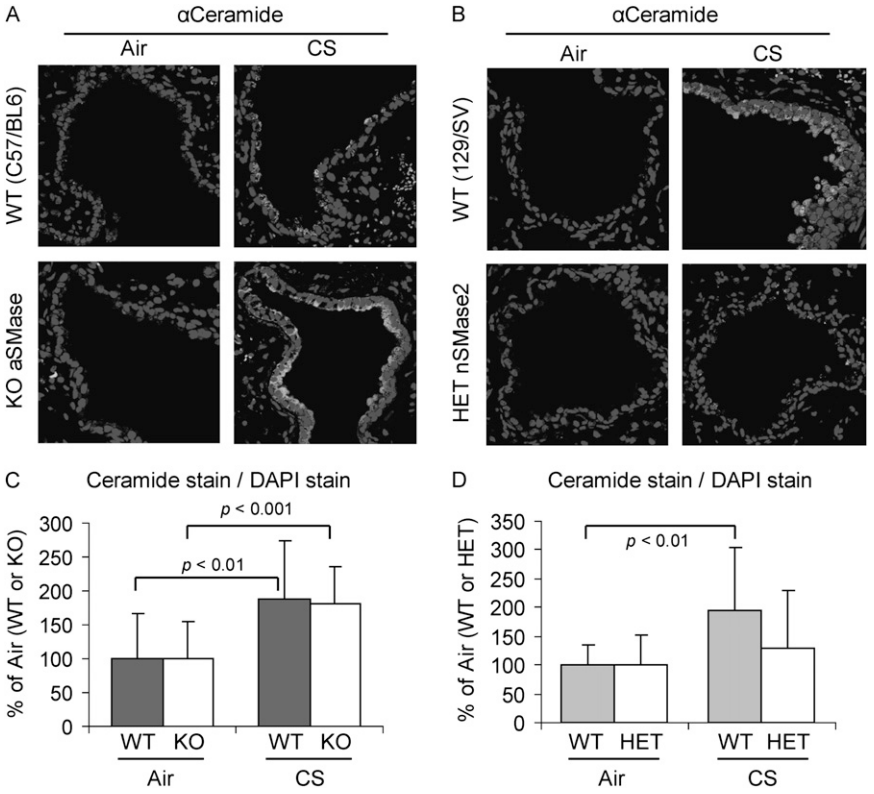

Figure 7. nSMase2, and not acidic sphingomyelinase (aSMase), is responsible for ceramide generation during CS exposure. Knockout (KO) mice for aSMase (*A*) and heterozygous (HET) mice for nSMase2 (nSMase2$^{-/+}$) (*B*) were exposed, or not, to CS for 3 weeks, killed, and assayed by IHC for ceramide levels in the lung sections using α-ceramide Ab, as in Figure 1 (*brighter stain*). Total nuclei were stained by DAPI. Images were acquired with an Olympus FluoView FV1000 laser scanning confocal microscope and show the merges of respective total nuclei and ceramide stains in filtered air (*left panels*) and CS-exposed (*right panels*) mice, for both KO aSMase (*A*) and HET nSMase2 (*B*), compared with the respective wild-type (WT) control animals (*upper panels*). (*C*) A total of 16 random images were acquired at 200× magnification from lung sections of 2 different mice per each treatment (8 images per each mouse), and the mean intensity of ceramide stain has been normalized to DAPI stain as in Figure 4 (i.e., the average values of ceramide stains from the air-exposed mice), for both WT and KO aSMase mice, were arbitrarily set as 100%, and other values (means and SDs) were adjusted. (*D*) Ceramide stains in lung sections of 129/Sv mice, WT, or HET nSMase2, were quantified as described in (*C*) and reported as means (±SD). The *P* values in (*C*) and (*D*) were obtained by Student's *t* test per number of images.

data suggest that the absence of nSMase2 reduces the susceptibility of the mice to CS exposure and ceramide production.

nSMase2 Expression in the Lungs of SHR Rats

Because of our experimental design using KO mice, we were constrained to use 129/Sv WT and C57BL/6 WT mice, the background strains for the KO and HET mice tested, for our experiments with mice. The SHR is a recognized model for a rodent strain that is genetically susceptible to COPD, and perhaps better represents the relatively low percentage of human smokers who develop COPD from smoking. Thus, we repeated some of our experiments in this rat strain. The results obtained in mice exposed to CS were substantiated in studies with rats (SHR/NCrIBR) that were exposed to CS for up to 14 weeks. The lung sections from the exposed rats were also stained for TUNEL-positive cells, and to determine the expression of nSMase2 protein. The pattern of changes obtained for the exposed rats was very similar to that shown previously here for the mice exposed to CS, and that could also be observed after 3–4 weeks of CS exposure. Figure 8A demonstrates staining of lung sections taken from the rats after 14 weeks of CS exposure (or not). A significant increase in TUNEL-positive cells was observed in CS-exposed rats (lower panels) in comparison to control animals (upper panels), which was also accompanied by colocalization of the apoptotic cells with overexpressed nSMase2 (Figure 8A, central panels).

Of note is that these changes occurred side by side with the readily observed histological changes of airway epithelial metaplasia. Images of intrapulmonary airways and tissue parenchyma after 14 weeks (Figure 8B, upper panels and lower panels, respectively) of CS-exposed rats demonstrate ongoing epithelial injury and repair, as well as epithelial metaplasia. The parenchyma shows a significant enlarging of the airspaces, suggestive of a destructive process that is likely to involve up-regulation of apoptosis (Figure 8B). These observations corroborate previous findings by others that have indicated that apoptosis and metaplasia take place at the same time, and may perhaps partially explain why patients with COPD have a higher incidence of lung cancer (34).

Moreover, increasing numbers of inflammatory cells (leukocytes, neutrophils, and macrophages) were recovered from the lungs of the SHR/NCrIBR rats by bronchoalveolar lavage after 3 days or 4 weeks of CS exposure (data not shown), demonstrating that the inflammatory component of COPD is also elevated in these rats.

As summarized in the model presented in Figure 8C, taken together, our recent data demonstrate that exposure of mice and rats to CS leads to elevated ceramide levels in the lung, followed by an increase in TUNEL-positive cells localized to the same areas of ceramide generation. All of these changes are specifically dependent on nSMase2 expression in the bronchial and alveolar epithelium.

nSMase2 Expression in the Lungs of Human Cigarette Smokers with Emphysema

We also examined lung sections from control humans and from smokers with clinically diagnosed and biopsy-verified emphysema, as shown in Figure 9, which presents staining of human lung biopsies with anti-nSMase2 antibody, both via colorimetric (Figure 9A) and fluorescent (Figure 9B) techniques. The human samples, provided by Dr. Rubin Tuder, demonstrated that patients with emphysema (smokers) have higher levels of nSMase2 expression in the alveolar spaces (Figure 9), suggesting a role for nSMase2 expression in patients with emphysema who smoke. Of special note is the apparent similarity of expression of nSMase2 in the human lungs and in the rodent lungs exposed to CS shown in Figures 2, 3, and 8.

DISCUSSION

Animal models using smoke exposure would appear to be very useful for investigation of the detailed molecular mechanisms

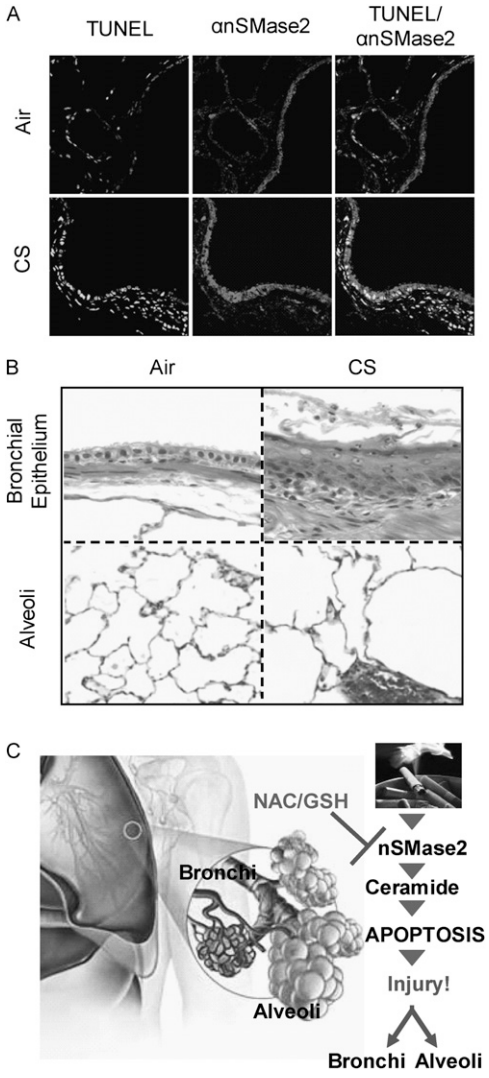

Figure 8. nSMase2 expression and TUNEL staining are augmented in lung of CS-exposed rats. Spontaneously hypertensive rat (SHR)/NCrIBR rats were exposed, or not, to CS. (*A*) Fragmented DNA was stained by TUNEL assay as in Figure 2 (*left panels*), and nSMase2 expression was evaluated by incubation with αnSMase2 Ab (*central panels*). Merge images of TUNEL and nSMase2 staining are shown in the *right panels.* Images were acquired with an Olympus FluoView FV1000 laser scanning confocal microscope. (*A*) Representative of images scored by four people independently, who analyzed random lung sections. (*B*) Lung sections stained by H&E showed epithelial metaplasia (*upper panels*) and parenchyma airspace enlargement (*lower panels*) after CS exposure: the epithelial lining of the airway in the filtered air control is composed of a simple cuboidal layer of ciliated and nonciliated cells (*upper left panel*). In contrast, exposure to tobacco smoke for 14 weeks is associated with a thickened, stratified squamous epithelium in the form of keratinizing squamation of the epithelium, with numerous inflammatory cells and debris in the airway lumen (*upper right panel*). The parenchyma (*lower panels*) show a significant enlargement of the airspaces of CS-exposed mice (*lower right panel*) in comparison to the filtered air-exposed control (*lower left panel*). The changes in airspace size are estimated to be increased approximately 50% above filtered air controls in mean linear intercept length within the airspaces of the lung parenchyma. (*C*) Model of CS-induced injury. CS exposure of airway cells specifically causes overexpression and activation of nSMase2, which leads to increased ceramide generation and occurrence of apoptosis, producing lung injury in both bronchial epithelium and alveoli. An antioxidant, such as NAC, precursor of glutathione (GSH), can quench the overexpression and activation of nSMase2, and thus reduce the occurrence of apoptosis.

responsible for the pathogenesis of COPD, but it is only relatively recently that such models have been created (35). Experiments in which animals have been chronically exposed to CS have provided some insights into strain differences in susceptibility among mice, as well as into disease pathogenesis (36–38). In the current study, we demonstrate, for the first time, that mice (129/Sv and C57BL/6 strains) or rats (SHR/NCrIBR) exposed to CS accumulate ceramide in the lung, and that this CS-induced accumulation can be mimicked by local instillation of synthetic membrane-permeant ceramide analogs (i.e., C6-ceramide). Moreover, we demonstrate that accumulation of ceramide colocalizes with increased numbers of TUNEL-positive cells. Using a new antibody generated in our laboratory against partially purified nSMase2, we also demonstrated by IHC that nSMase2 expression was elevated both in the bronchial epithelium and in the alveoli of the lungs of mice or rats exposed to CS for several weeks. Ceramide elevation and increased numbers of TUNEL-positive cells were localized to the same lung areas as nSMase2 protein overexpression, suggesting that all three of these steps in lung injury are coordinated. Furthermore, we have also observed increased expression of nSMase2 in the lungs of human smokers with emphysema. Because nSMase2 is a novel target, the relative stability of the protein and the message levels under CS exposure are still unknown. It is feasible that the expression of nSMase2 is regulated both at the transcriptional level and at the post-translational level; these possibilities are currently under investigation (unpublished observations).

Our studies demonstrate for the first time that exposure to CS leads to ceramide generation and excessive apoptosis induction in mice and rats through the specific activation of nSMase2, which can be quenched by pretreatment of mice with NAC. Ceramide levels were not elevated in lung sections from mice after CS exposure when nSMase2 was locally silenced by siRNA. This finding confirmed unequivocally that nSMase2 is indeed the specific target modulated by CS to promote ceramide production in the lung. Further studies in KO mice corroborated the findings that only nSMase2, and not aSMase, is the target of CS exposures, highlighting the essential role of nSMase2 in ceramide generation and apoptosis augmentation in lung injury under CS exposure. These results suggest that overexpression of nSMase2 may be a putative cause for the initiation or progression of CS-induced lung diseases.

nSMase2 was previously found in the brain (39), and recent reports presented a role for nSMase2 in aging (40) and in Alzheimer's disease (41). At the same time, we have shown that reactive oxidants up-regulate ceramide generation and cause pathological cell death in HAE cells (15, 19, 29, 42). We thus proposed that there must be a specific SMase that is modulated by ROS in lung epithelial cells. This led to the isolation of the novel nSMase2 from monkey lung tissue and from HAE cells (42). We then presented (19, 42) that, when nSMase2 was siRNA silenced, lung epithelial cells could not undergo cell death in response to ROS or CS exposure, suggesting that nSMase2 could be a critical target not only in the brain pathogenesis, but also in ROS-/CS-induced lung injury in respiratory diseases.

It is presently unknown whether the overexpression of nSMase2 observed *in vivo* is under transcriptional regulation or due to enhanced stabilization mechanisms of the protein itself. However, it appears that the nSMase2 up-regulation is mediated by oxidative stress exerted by CS. A diet enriched with NAC,

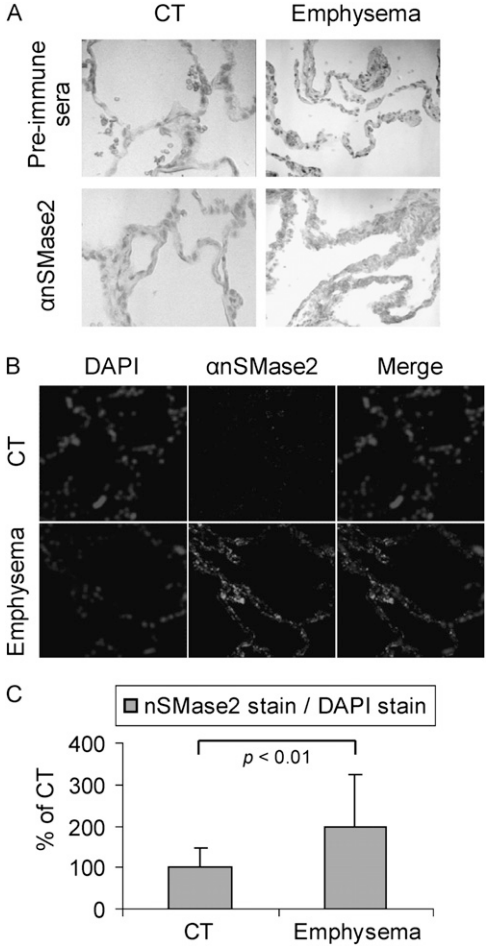

Figure 9. nSMase2 expression is augmented in lung tissue from patients with emphysema. Lung tissue sections were incubated with αnSMase2 Ab or the preimmune sera (rabbit). Images were acquired by optical microscopy after colorimetric staining by incubating with avidin–biotin complex Ab and DAB (*A*), or with an LSM 5 Pascal Zeiss laser scanning confocal microscope after staining αnSMase2 by Alexa Fluor 555 dye (*central panels*) (*B*). (*A*) Representative of images scored by four people independently, who analyzed random lung sections from control subjects (CTs) or patients with emphysema. (*B*) Total nuclei were stained by DAPI and merged with images of nSMase2 expression. The *histogram* in (*C*) shows the quantification of nSMase2 staining in the fluorescent experiments. A total of 16 random images was acquired at 200× magnification from lung sections of 2 different CTs and patients with emphysema (8 images per patient), then the mean intensity of nSMase2 stain was normalized to DAPI stain, as in Figure 4. The average value of nSMase2 stains of the CTs was arbitrarily set as 100%, and the other values (means and SDs) were adjusted. The *P* value was obtained by Student's *t* test per number of images.

a well known antioxidant molecule (30), significantly reduced both the over expression of nSMase2 and apoptosis. Indeed, we reported recently that H_2O_2-oxidative stress generated by CS is the specific cause for nSMase2 activation in HAE cells. Moreover, generation of ceramide in response to CS/H_2O_2 exposures was abolished by antioxidants, such as GSH and NAC (14, 16, 19, 42, 43). Consistent with these observations, the same antioxidants were also shown by others to inhibit nSMase activity and ceramide generation in different cell lines (44, 45). Moreover, it is known that a diet with NAC can restore GSH depletion in the lung and prevent the oxidative stress–induced injury (46).

aSMase was the first SMase to be shown to have a role in a disease (47), as types A and B Niemann-Pick disease result from the deficient activity of aSMase. Recent reports point toward aSMase as the target responsible for ceramide generation in various pathologies (6, 9, 10, 23). Although a role for the lysosomal aSMase has been described in edema (48), and also suggested to play a role in other pulmonary pathologies, such as cystic fibrosis (9, 49) and emphysema (5), our data suggest that it is nSMase2 that serves as an exclusive target to generate ceramide under the stress of CS exposure. nSMase2$^{-/+}$ mice present a reduction of ceramide accumulation in comparison to WT mice when exposed to CS; on the other hand, aSMase$^{-/-}$ mice could accumulate ceramide under CS exposure as much as the WT mice, demonstrating that only nSMase2, and not aSMase, is modulated by CS. This finding is consistent with our previous observations in HAE cells, which showed that CS and H_2O_2-oxidative stress specifically activate nSMase2, and not aSMase (14, 19, 29).

Oxidative stress–generated ceramide has been connected to activation of nSMase and not aSMase in different cell lines, suggesting a role for nSMase activity in pathogenesis of other diseases, such as multiple sclerosis, hepatic failure (50, 51), aging (45), and Alzheimer's disease (41). We do not exclude the possibility that aSMase may also have a role in emphysema or other pulmonary pathologies (49); however, our studies in airway epithelial cells (19, 42) and the studies presented here in mice show clearly that only nSMase2, and not aSMase, is activated by oxidative stress and CS exposure. Furthermore, using our newly developed anti-nSMase2 antibody, we were also able to demonstrate, for the first time, that lung tissues from patients with emphysema (smokers) display high levels of nSMase2 expression compared with normal patients. Therefore, nSMase2, a member of the ceramide-generating machinery, presents a potential novel target in the prevention of CS-induced apoptosis in lung epithelial cells, the initiation step of epithelial/alveoli injury in COPD.

The molecular mechanism that links CS and/or oxidative stress to augmented nSMase2 expression and activity is far from being completely understood. We have recently shown that nSMase2 is a phosphoprotein in which the level of phosphorylation is modulated by oxidative stress, which also controls nSMase2 function (52).

In summary, nSMase2 is specifically activated by the ROS (particularly H_2O_2) component of CS, thereby increasing ceramide generation via hydrolysis of sphingomyelin, and thus elevating pathological apoptosis in the lung epithelium, which enhances lung injury. GSH blocks these effects of CS. The pathological apoptosis is shown now not only in airway epithelial cells (19, 29, 42), but also in the bronchi and alveoli of mice and rats, and the link to nSMase2 up-regulation may also contribute to lung injury in human smokers. Our results with nSMase2$^{-/+}$ mice, aSMase$^{-/-}$ mice, and siRNA silencing of nSMase2 in WT mice demonstrate that only nSMase2, and not aSMase, is modulated by CS. Moreover, samples from humans demonstrated that patients with emphysema (smokers) have substantially higher levels of nSMase2 expression in the alveolar spaces than control patients. Of special significance is the noticeable resemblance of elevated nSMase2 expression in the lungs of rodents exposed to CS. Therefore, with such a role in lung epithelial apoptosis/injury, nSMase2, a member of the ceramide-generating machinery, may be an attractive and specific target for the prevention of the airway destruction that is the hallmark of CS-induced emphysema.

Author Disclosure: E.K. has received a training grant from the National Institutes of Health (NIH) ($10,001–$50,000); J.L. has received sponsored grants from the NIH (more than $100,000) and from Phillip Morris External Research Program (2001–2004, more than $100,000) for researching mechanisms of interactions of air pollutants and airway remodeling in asthma; K.P. received industry-sponsored

grants from AstraZeneca (more than $100,000), and has received sponsored grants from Philip Morris (2003–2007, more than $100,000) to examine a model of chronic obstructive pulmonary disease in the spontaneously hypertensive rat, with an emphasis on elucidating the mechanisms of tobacco smoke–induced inflammation and injury to the conducting airways—K.P. confirms that no funds were received from Philip Morris for experiments described in this manuscript; no experiments described in this manuscript were performed using funds from Philip Morris; N.K. has served on the advisory board for California Chronic Disease Management/California Medical Association (less than $1,000); T.G. has received reimbursement for consultancies from Novartis (less than $1,000) and sponsored grants from the NIH (more than $100,000); none of the other authors has a financial relationship with a commercial entity that has an interest in the subject of this manuscript.

References

1. Yoshida T, Tuder RM. Pathobiology of cigarette smoke–induced chronic obstructive pulmonary disease. *Physiol Rev* 2007;87:1047–1082.
2. Churg A, Wright JL. Proteases and emphysema. *Curr Opin Pulm Med* 2005;11:153–159.
3. Demedts IK, Demoor T, Bracke KR, Joos GF, Brusselle GG. Role of apoptosis in the pathogenesis of COPD and pulmonary emphysema. *Respir Res* 2006;7:53.
4. Giordano RJ, Lahdenranta J, Zhen L, Chukwueke U, Petrache I, Langley RR, Fidler IJ, Pasqualini R, Tuder RM, Arap W. Targeted induction of lung endothelial cell apoptosis causes emphysema-like changes in the mouse. *J Biol Chem* 2008;283:29447–29460.
5. Petrache I, Natarajan V, Zhen L, Medler TR, Richter AT, Cho C, Hubbard WC, Berdyshev EV, Tuder RM. Ceramide upregulation causes pulmonary cell apoptosis and emphysema-like disease in mice. *Nat Med* 2005;11:491–498.
6. Petrache I, Medler TR, Richter AT, Kamocki K, Chukwueke U, Zhen L, Gu Y, Adamowicz J, Schweitzer KS, Hubbard WC, *et al.* Superoxide dismutase protects against apoptosis and alveolar enlargement induced by ceramide. *Am J Physiol Lung Cell Mol Physiol* 2008;295: L44–L53.
7. Claus R, Bunck A, Bockmeyer C, Brunkhorst F, Losche W, Kinscherf R, Deigner H. Role of increased SMase activity in apoptosis and organ failure of patients with severe sepsis. *Faseb J* 2005;19:1719–1721.
8. Masini E, Giannini L, Nistri S, Cinci L, Mastroianni R, Xu W, Comhair SA, Li D, Cuzzocrea S, Matuschak GM, *et al.* Ceramide: a key signaling molecule in a guinea pig model of allergic asthmatic response and airway inflammation. *J Pharmacol Exp Ther* 2008;324:548–557.
9. Teichgraber V, Ulrich M, Endlich N, Riethmuller J, Wilker B, De Oliveira-Munding CC, van Heeckeren AM, Barr ML, von Kurthy G, Schmid KW, *et al.* Ceramide accumulation mediates inflammation, cell death and infection susceptibility in cystic fibrosis. *Nat Med* 2008; 14:382–391.
10. Hamai H, Keyserman F, Quittell LM, Worgall TS. Defective CFTR increases synthesis and mass of sphingolipids that affect membrane composition and lipid signaling. *J Lipid Res* 2009;50:1101–1108.
11. Gulbins E, Li PL. Physiological and pathophysiological aspects of ceramide. *Am J Physiol Regul Integr Comp Physiol* 2006;290:R11–R26.
12. Dbaibo GS, Hannun YA. Signal transduction and the regulation of apoptosis: roles of ceramide. *Apoptosis* 1998;3:317–334.
13. Goldkorn T, Ravid T, Khan EM. Life and death decisions: ceramide generation and EGF receptor trafficking are modulated by oxidative stress. *Antioxid Redox Signal* 2005;7:119–128.
14. Chan C, Goldkorn T. Ceramide path in human lung cell death. *Am J Respir Cell Mol Biol* 2000;22:460–468.
15. Goldkorn T, Balaban N, Shannon M, Chea V, Matsukuma K, Gilchrist D, Wang H, Chan C. H_2O_2 acts on cellular membranes to generate ceramide signaling and initiate apoptosis in tracheobronchial epithelial cells. *J Cell Sci* 1998;111:3209–3220.
16. Lavrentiadou SN, Chan C, Ravid T, Tsaba A, van der Vliet A, Rasooly R, Goldkorn T. Ceramide-mediated apoptosis in lung epithelial cells is regulated by GSH. *Am J Respir Cell Mol Biol* 2001;25:676–684.
17. Ravid T, Tsaba A, Gee P, Rasooly R, Medina EA, Goldkorn T. Ceramide accumulation precedes caspase-3 activation during apoptosis of A549 human lung adenocarcinoma cells. *Am J Physiol Lung Cell Mol Physiol* 2003;284:L1082–L1092.
18. Hannun YA, Obeid LM. The ceramide-centric universe of lipid-mediated cell regulation: stress encounters of the lipid kind. *J Biol Chem* 2002;277:25847–25850.
19. Levy M, Khan E, Careaga M, Goldkorn T. Neutral sphingomyelinase 2 is activated by cigarette smoke to augment ceramide-induced apoptosis in lung cell death. *Am J Physiol Lung Cell Mol Physiol* 2009; 297:125–133.
20. Park JW, Ryter SW, Choi AM. Functional significance of apoptosis in chronic obstructive pulmonary disease. *COPD* 2007;4:347–353.
21. Henson PM, Vandivier RW, Douglas IS. Cell death, remodeling, and repair in chronic obstructive pulmonary disease? *Proc Am Thorac Soc* 2006;3:713–717.
22. Elias J, Kang M, Crothers K, Homer R, Lee C. State of the art. Mechanistic heterogeneity in chronic COPD: insights from transgenic mice. *Proc Am Thorac Soc* 2006;3:494–498.
23. Uhlig S, Gulbins E. Sphingolipids in the lungs. *Am J Respir Crit Care Med* 2008;178:1100–1114.
24. Zhang X, Shan P, Jiang D, Noble PW, Abraham NG, Kappas A, Lee PJ. Small interfering RNA targeting heme oxygenase−1 enhances ischemia–reperfusion–induced lung apoptosis. *J Biol Chem* 2004; 279:10677–10684.
25. Krishnamurthy K, Dasgupta S, Bieberich E. Development and characterization of a novel anti-ceramide antibody. *J Lipid Res* 2007;48:968–975.
26. Jaffrezou JP, Maestre N, de Mas-Mansat V, Bezombes C, Levade T, Laurent G. Positive feedback control of neutral sphingomyelinase activity by ceramide. *FASEB J* 1998;12:999–1006.
27. Contreras FX, Basanez G, Alonso A, Herrmann A, Goni FM. Asymmetric addition of ceramides but not dihydroceramides promotes transbilayer (flip-flop) lipid motion in membranes. *Biophys J* 2005;88: 348–359.
28. Noe J, Petrusca D, Rush N, Deng P, Vandemark M, Berdyshev E, Gu Y, Smith P, Schweitzer K, Pilewsky J, *et al.* CFTR regulation of intracellular ph and ceramides is required for lung endothelial cell apoptosis. *Am J Respir Cell Mol Biol* 2009;41:314–323.
29. Castillo SS, Levy M, Thaikoottathil JV, Goldkorn T. RNS and ROS activate different SMases to induce apoptosis in airway epithelial cells. *Exp Cell Res* 2007;313:2680–2686.
30. Prakash A, Kumar A. Effect of N-acetyl cysteine against aluminium-induced cognitive dysfunction and oxidative damage in rats. *Basic Clin Pharmacol Toxicol* 2009;61:1665–1672.
31. Balansky R, Ganchev G, Iltcheva M, Steele VE, De Flora S. Prenatal N-acetylcysteine prevents cigarette smoke–induced lung cancer in neonatal mice. *Carcinogenesis* 2009;30:1398–1401.
32. Sultan I, Senkal CE, Ponnusamy S, Bielawski J, Szulc Z, Bielawska A, Hannun YA, Ogretmen B. Regulation of the sphingosine-recycling pathway for ceramide generation by oxidative stress, and its role in controlling c-Myc/Max function. *Biochem J* 2006;393:513–521.
33. Hughes SE. Detection of apoptosis using *in situ* markers for DNA strand breaks in the failing human heart: fact or epiphenomenon? *J Pathol* 2003;201:181–186.
34. Koshiol J, Rotunno M, Consonni D, Pesatori AC, De Matteis S, Goldstein AM, Chaturvedi AK, Wacholder S, Landi MT, Lubin JH, *et al.* Chronic obstructive pulmonary disease and altered risk of lung cancer in a population-based case–control study. *PLoS ONE* 2009;4: e7380.
35. Wright JL, Cosio M, Churg A. Animal models of chronic obstructive pulmonary disease. *Am J Physiol Lung Cell Mol Physiol* 2008;295:L1–L15.
36. March TH, Wilder JA, Esparza DC, Cossey PY, Blair LF, Herrera LK, McDonald JD, Campen MJ, Mauderly JL, Seagrave J. Modulators of cigarette smoke–induced pulmonary emphysema in a/j mice. *Toxicol Sci* 2006;92:545–559.
37. March TH, Bowen LE, Finch GL, Nikula KJ, Wayne BJ, Hobbs CH. Effects of strain and treatment with inhaled all-trans-retinoic acid on cigarette smoke–induced pulmonary emphysema in mice. *COPD* 2005;2:289–302.
38. Groneberg DA, Chung KF. Models of chronic obstructive pulmonary disease. *Respir Res* 2004;5:18.
39. Hofmann K, Tomiuk S, Wolff G, Stoffel W. Cloning and characterization of the mammalian brain-specific, Mg^{2+}-dependent neutral sphingomyelinase. *Proc Natl Acad Sci USA* 2000;97:5895–5900.
40. Rutkute K, Asmis RH, Nikolova-Karakashian MN. Regulation of neutral sphingomyelinase-2 by GSH: a new insight to the role of oxidative stress in aging-associated inflammation. *J Lipid Res* 2007;48: 2443–2452.
41. Satoi H, Tomimoto H, Ohtani R, Kitano T, Kondo T, Watanabe M, Oka N, Akiguchi I, Furuya S, Hirabayashi Y, *et al.* Astroglial expression of ceramide in Alzheimer's disease brains: a role during neuronal apoptosis. *Neuroscience* 2005;130:657–666.
42. Levy M, Castillo SS, Goldkorn T. nSMase2 activation and trafficking are modulated by oxidative stress to induce apoptosis. *Biochem Biophys Res Commun* 2006;344:900–905.

43. Goldkorn T, Khan EM. Dual roles of oxidative stress in the lungs. In: Valacchi G, Davis PA, editors. editor. Oxidants in biology: a question of balance. The Netherlands: Springer; 2008. pp. 231–250.
44. Okamoto Y, Obeid LM, Hannun YA. Bcl-xL interrupts oxidative activation of neutral sphingomyelinase. *FEBS Lett* 2002;530:104–108.
45. Rutkute K, Karakashian AA, Giltiay NV, Dobierzewska A, Nikolova-Karakashian MN. Aging in rat causes hepatic hyperresposiveness to IL-1beta which is mediated by nSMase2. *Hepatology* 2007;46:1166–1176.
46. Li J, Wang H, Stoner GD, Bray TM. Dietary supplementation with cysteine prodrugs selectively restores tissue glutathione levels and redox status in protein-malnourished mice(1). *J Nutr Biochem* 2002; 13:625–633.
47. Horinouchi K, Erlich S, Perl DP, Ferlinz K, Bisgaier CL, Sandhoff K, Desnick RJ, Stewart CL, Schuchman EH. Acid sphingomyelinase deficient mice: a model of types A and B Niemann-Pick disease. *Nat Genet* 1995;10:288–293.
48. Goggel R, Winoto-Morbach S, Vielhaber G, Imai Y, Lindner K, Brade L, Brade H, Ehlers S, Slutsky AS, Schutze S, *et al.* PAF-mediated pulmonary edema: a new role for acid sphingomyelinase and ceramide. *Nat Med* 2004;10:155–160.
49. Smith EL, Schuchman EH. The unexpected role of acid sphingomyelinase in cell death and the pathophysiology of common diseases. *FASEB J* 2008;22:3419–3431.
50. Ichi I, Kamikawa C, Nakagawa T, Kobayashi K, Kataoka R, Nagata E, Kitamura Y, Nakazaki C, Matsura T, Kojo S. Neutral sphingomyelinase–induced ceramide accumulation by oxidative stress during carbon tetrachloride intoxication. *Toxicology* 2009;261:33–40.
51. Jana A, Pahan K. Oxidative stress kills human primary oligodendrocytes via neutral sphingomyelinase: implications for multiple sclerosis. *J Neuroimmune Pharmacol* 2007;2:184–193.
52. Filosto S, Fry W, Knowlton AA, Goldkorn T. Neutral sphingomyelinase2 (nSMase2) is a phosphoprotein regulated by calcineurin (PP2B). *J Biol Chem* 2010;285:10213–10222.